AD-A179 187   TELESEISMIC WAVEFORM MODELING INCORPORATING THE EFFECTS   1/1
               OF KNOWN THREE-DI..(U) MASSACHUSETTS INST OF TECH
               CAMBRIDGE EARTH RESOURCES LAB U F CORMIER 02 JAN 87
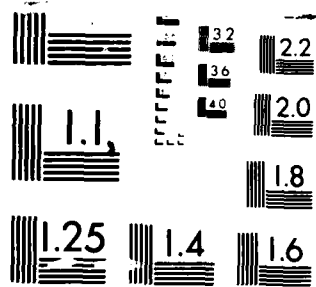UNCLASSIFIED   AFGL-TR-87-0037 F19628-85-K-0031   F/G 8/11   NL

END
DATE
FILMED
5 87

MICROCOPY RESOLUTION TEST CHART
NATIONAL BUREAU OF STANDARDS 1963-A

⑫

AD-A179 187

AFGL-TR-87-0037

TELESEISMIC WAVEFORM MODELING INCORPORATING THE
EFFECTS OF KNOWN THREE-DIMENSIONAL STRUCTURE
BENEATH THE NEVADA TEST SITE

Vernon F. Cormier

Massachusetts Institute of Technology
Earth Resources Laboratory
Department of Earth, Atmospheric, and
  Planetary Sciences
Cambridge, MA 02139

2 January 1987

Scientific Report No. 3

DTIC
ELECTE
S APR 2 0 1987
E
D

87 4 17 080

"This technical report has been reviewed and is approved for publication"

JAMES F. LEWKOWICZ
Contract Manager

HENRY A. OSSING
Branch Chief

FOR THE COMMANDER

DONALD H. ECKHARDT
Division Director

This report has been reviewed by the ESD Public Affairs Office (PA) and is releasable to the National Technical Information Service (NTIS).

Qualified requestors may obtain additional copies from the Defense Technical Information Center. All others should apply to the National Technical Information Service.

If your address has changed, or if you wish to be removed from the mailing list, or if the addressee is no longer employed by your organization, please notify AFGL/DAA, Hanscom AFB, MA 01731. This will assist us in maintaining a current mailing list.

Do not return copies of this report unless contractual obligations or notices on a specific document requires that it be returned.

REPORT DOCUMENTATION PAGE

1a REPORT SECURITY CLASSIFICATION Unclassified	1b. RESTRICTIVE MARKINGS

2a SECURITY CLASSIFICATION AUTHORITY	3. DISTRIBUTION / AVAILABILITY OF REPORT
2b. DECLASSIFICATION / DOWNGRADING SCHEDULE	Approved for public release; distribution unlimited

4. PERFORMING ORGANIZATION REPORT NUMBER(S)	5. MONITORING ORGANIZATION REPORT NUMBER(S) AFGL-TR-87-0037

6a. NAME OF PERFORMING ORGANIZATION Earth Resources Laboratory Dept. of Earth, Atmospheric, and Planetary Sciences	6b. OFFICE SYMBOL (If applicable)	7a. NAME OF MONITORING ORGANIZATION Air Force Geophysics Laboratory

6c. ADDRESS (City, State, and ZIP Code) Massachusetts Institute of Technology Cambridge, MA 02139	7b. ADDRESS (City, State, and ZIP Code) Hanscom Air Force Base Massachusetts 01731

8a. NAME OF FUNDING / SPONSORING ORGANIZATION Air Force Geophysics Laboratory	8b. OFFICE SYMBOL (If applicable)	9 PROCUREMENT INSTRUMENT IDENTIFICATION NUMBER F19628-85-K-0031

8c. ADDRESS (City, State, and ZIP Code) Hanscom Air Force Base Massachusetts 01731 J. Lewkowicz/LWH	10 SOURCE OF FUNDING NUMBERS			
	PROGRAM ELEMENT NO 61101E	PROJECT NO 5A10	TASK NO DA	WORK UNIT ACCESSION NO AJ

11 TITLE (Include Security Classification)
Teleseismic Waveform Modeling Incorporating the Effects of Known Three-Dimensional
Structure Beneath the Nevada Test Site

12 PERSONAL AUTHOR(S)
Vernon F. Cormier

13a TYPE OF REPORT Technical Report No. 3	13b. TIME COVERED FROM 2/1/86 TO 7/31/86	14. DATE OF REPORT (Year, Month, Day) 2 January 1987	15 PAGE COUNT 30

16. SUPPLEMENTARY NOTATION

17	COSATI CODES		18 SUBJECT TERMS (Continue on reverse if necessary and identify by block number)
FIELD	GROUP	SUB-GROUP	seismic body waves, focusing, defocusing, yield estimation

19 ABSTRACT (Continue on reverse if necessary and identify by block number)
The focusing and defocusing of teleseismic P waves predicted by a known (Taylor,
1983) three-dimensional structure beneath the Nevada Test Site is calculated by dynamic
ray tracing and superposition of Gaussian beams. The 20 to 100 km scale lengths of this
model, having velocity fluctuations of several per cent, account for a factor of three
fluctuations in the azimuthal pattern of P amplitudes. Since similar sized scale lengths
and intensities of velocity fluctuation are commonly resolved in three-dimensional
inversions of mantle structure in other regions, focusing and defocusing of teleseismic
P waves is likely to be a ubiquitous feature of every test site. Hence, network averages
of m_b that weight azimuthal windows, in which P energy is either focused or defocused, will
tend to either over or under estimate the yields of underground tests. The results
obtained with a known NTS structure suggest that structural inversions having similar
structural resolution may be capable of reducing 25 per cent of the variance in amplitudes
due to the focusing and defocusing of upper mantle structure near the source.

20. DISTRIBUTION / AVAILABILITY OF ABSTRACT ☒ UNCLASSIFIED/UNLIMITED ☐ SAME AS RPT ☐ DTIC USERS	21 ABSTRACT SECURITY CLASSIFICATION Unclassified
22a. NAME OF RESPONSIBLE INDIVIDUAL James F. Lewkowicz	22b. TELEPHONE (Include Area Code) 617/861-3028 | 22c. OFFICE SYMBOL LWH

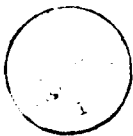**DD FORM 1473, 84 MAR**   83 APR edition may be used until exhausted.   SECURITY CLASSIFICATION OF THIS PAGE
All other editions are obsolete

19. (continued)

·Assuming that scattering processes are concentrated in the crust and uppermost mantle beneath the source and receiver, the integrated energy in the P coda should be more stable than direct P, because it tends to homogenize the effect of focusing/ defocusing structure near the source for scattering into direct P near the source. For direct P scattering near the receiver, however, even the late coda is not capable of completely removing the effects of focusing/defocusing near the source.

INTRODUCTION

The underground nuclear tests conducted in the Pahute Mesa region of the Nevada Test Site (Figure 1) exhibit a unique and reproducible azimuthal pattern in the amplitudes of short period P waves at teleseismic range (Lay et al. 1984). Because this pattern differs from those of tests conducted in other regions of the test site. it cannot simply be explained by either receiver effects or by variations in intrinsic attenuation along different paths in the mantle.

Evidence of tectonic release in the waveforms of long period P and S waves of large (greater than 500 kt.) Pahute events (Wallace et al. 1983. 1984), suggests that tectonic release may be the mechanism that also produces the azimuthal variation of the amplitude of short period P waves. A study by Lay et al (1984) initially favored this explanation, but noted the difficulty in formulating a physically realizable mechanism of tectonic release that would be capable of strongly affecting short period amplitudes. The required tectonic event would have to occur nearly simultaneously with the explosion. Theoretical and model studies of the relaxation of the likely pre-stress in this region have found negligible effects on the amplitudes of short period P waves (Archambeau. 1972; Bache. 1975).

More recent studies by Lynnes and Lay (1984) and Lay and Welc (1986a) hypothesize that the azimuthal pattern of amplitudes from Pahute tests instead caused focusing and defocusing of P waves by three-dimensional structure in the mantle beneath the test site. The mantle structure resolved in the inversions of Minster et al (1981) and Montfort and Evans (1982) are too broad in scale length and too weak in per cent velocity fluctuation to have much of an effect on the focusing and defocusing of teleseismic P waves. Hence. the approach followed by Lynnes and Lay was to find an ad-hoc structure consistent with the observed pattern of amplitudes. The resulting structure bore some resemblance to a high velocity anomaly mapped in the mantle northeast of Pahute Mesa in a travel time inversion by Taylor et al (1983). The effects of

1

the structure resolved in the Taylor model, however, were not directly investigated.

This paper will report on the results of forward modeling of teleseismic P waves for an explosive point source placed in the Taylor (1983) model at a Pahute hypocenter. Direct calculation of the focusing and defocusing effects of the Taylor model is relevant to reducing the uncertainties in the yield estimates of underground tests for several reasons. First, the model would be representative of the best information that would likely be obtainable at foreign test sites, short of deploying dense local arrays within the test site. Comparable data needed to obtain similar resolution of structure would consist of a regional array located primarily outside the test site and a well distributed set of tests with known origin times and hypocenters. Second, the effects of a known model for the structure beneath Pahute Mesa can aid in identifying any biasing effects of focusing and defocusing on the construction of empirical yield versus m_b curves from NTS data. For example, if globally averaged m_b's are concentrated in a narrow azimuthal band of focused or defocused energy, then yields from Pahute events will provide points to the empirical curve that are either biased toward high or low yield.

EFFECTS ON DIRECT P

Seismograms of teleseismic P waves were synthesized for sources in the Taylor model using the techniques described in Cormier (1986). The model was specified on a three-dimensional grid by per cent perturbations from a reference model. Only those perturbations were used whose diagonal elements of the resolution matrix exceeded 0.6. Continuous first and second spatial derivatives of velocity were calculated from splines under tension. Ray tracing was performed by integrating the kinematic and dynamic equations numerically in the three-dimensional region surrounding the source, and analytically along the rest of the ray path in a flattened, radially symmetric earth model. Seismograms were calculated both by simple ray theory and by superposition of Gaussian beams (Červený, 1985a,b).

2

Gaussian beam modeling Superposition of Gaussian beams was first performed in order to check whether the three-dimensional model was capable of producing any frequency dependent effects at teleseismic range. Gaussian beams remain regular at caustics and can succeed in predicting the first order effects of frequency dependence at caustics. The beam superposition also averages the effects of structural scale lengths that are small with respect to wavelength. (Here. structural scale length is taken to mean the distance between local minima and maxima of velocity perturbation.) Beam width parameters were chosen as described in Cormier (1986), which amounted to taking a plane wave superposition at the receivers with very wide Gaussian windowing.

Broadband, WWSSN short period. and WWSSN long period seismograms were synthesized for variable azimuths at a fixed receiver distance of 60° for a Pahute Mesa source located as shown in Figure 1. The synthetic seismograms (Figure 2) show little evidence of frequency dependence, with the relative amplitudes of waveforms in the three pass bands being nearly identical. Similar results were found in a study of a three-dimensional model having similar resolution and scale lengths of structure (Cormier, 1986). Amplitudes vary azimuthally by a factor of three, with the smallest amplitude being at the calculated due north azimuth. Figure 1 shows that ray paths in northerly directions will traverse a high velocity anomaly located in the mantle north of the epicenter. The associated travel time variation of several tenths of a second is too small to be easily visible in the synthetics. The sense of the travel time variation is consistent with focusing and defocusing: small amplitudes correlate with fast times, and large amplitudes with slow times. This correlation is discussed and shown in finer detail in the following section discussing the results of ray theoretical modeling.

Ray theoretical modeling Since the Gaussian beam modeling exhibited little evidence of frequency dependence, it was deemed appropriate to model seismograms by ray theory. Ray theoretical amplitudes were predicted from geometric **spreading** calculated from the determinant of the **Q** matrix obtained from dynamic **ray** tracing (e.g., Cerveny, 1985b). A dense system of rays was shot at variable vertical take-off

3

angles and azimuthal angles. The determinant of the $\mathbf{Q}$ matrix was evaluated at end points of the rays at the earth's surface. The ray theoretical amplitude is then equal to $\frac{1}{\sqrt{\det \mathbf{Q}}}$. Figure 3 plots these amplitudes versus azimuth for the system of rays shot. All amplitudes were normalized for the spreading factor appropriate for a P wave at 60° in a radially symmetric earth. The azimuth plotted is the azimuth at a point at which a ray leaves the three-dimensional region surrounding the source.

Note the pronounced minimum in amplitudes again occurs at northerly azimuths, with more steeply dipping rays at longer distances having the smallest amplitudes. A region of larger amplitudes occurs around -70° azimuth. In other azimuthal ranges, amplitudes scatter depending on the vertical take-off angle.

The large scatter around -30° azimuth is due to the presence of a caustic. The Gaussian beam synthesis did not test this azimuthal range. Calculations with other three-dimensional models obtained from block inversion of travel times and with statistically generated models find that such caustics can be easily generated by velocity perturbations as small as one per cent (Cormier, 1986; McLaughlin and Anderson, 1987). Tests with seismograms synthesized by superposition of Gaussian beams find only a very small amount of phase distortion in the P waves of receivers located near the caustic. This is because the class of caustic created by these models encloses a very small area on the earth's surface. This area is generally so small in the vicinity of the receiver that any phase distortion or frequency dependence in the waveforms is barely visible within the pass bands of common seismographs

Comparison of predicted with observed amplitudes Figure 4 shows observed amplitudes of Pahute events collected by Lay *et al* (1984). Note that the amplitude minimum predicted by the Taylor model at northerly azimuths is qualitatively matched. There is some match of the predicted maximum near -70° azimuth as well as of the form of the scatter between 50° to 150° azimuth. The minimum in the observed amplitudes is displaced slightly to the east of the predicted amplitudes. It appears that the high

4

velocity anomaly in the Taylor model is placed at about the right distance from the center of Pahute Mesa, but is displaced to the west relative to the true anomaly. This may be due to ray bending in the vicinity of the source, which the inversion technique ignores. Even without any azimuthal shift in the predicted amplitudes, the predicted amplitudes can be used to correct for focusing and defocusing giving about a 25 per cent reduction in variance in corrected log amplitudes. It is interesting to note that Taylor's model predicts a similar variance reduction in travel time anomalies. This suggests that a particular model's success in reducing the variance in travel times can be taken as a rough measure of its potential success in reducing the variance in log amplitudes due to focusing and defocusing.

The strong concentration of observations around the amplitude minimum will tend to reduce the network averaged m_b of Pahute events. This effect can to some extent be alleviated by more sophisticated measures of network averaged m_b, averaged of m_b, such as maximum likelihood (Ringdal, 1976). Maximum likelihood processing can take into account variations in the azimuthal distribution of stations and can be designed to provide azimuthally dependent weights based on the focusing and defocusing properties of the source region.

The dependence of focusing and defocusing effects on vertical as well as azimuthal ray angle is better illustrated in a plot of amplitudes on a focal sphere. This is shown in Figure 5. In this plot, the agreement between observed and predicted amplitudes is more compelling, with some second order features that depend on both take-off angles highlighted. Note the agreement of negative anomalies near azimuths 75°, 120°, 150°, and 190°, as well as the relative size of negative and positive anomalies in the northeast quadrant.

Correlation of predicted travel times and amplitudes. Figure 6 shows the azimuthal and take-off angle dependence of travel time residual predicted by Taylor's model. The same results are shown in the form of focal sphere plots in Taylor's paper. The residual

5

is taken from the predicted time of PREM (Dziewonski and Anderson, 1981). Figure 7 plots this travel time residual against amplitude. The general sense of the correlation expected for focusing and defocusing is apparent, with slow times correlating with large amplitudes. The scatter from this trend, however, is large. Thus, weak or nonexistent correlation of travel time anomalies with amplitude anomalies of data should not necessarily be taken as proof that focusing and defocusing are not affecting amplitudes.

An example of the relative behavior of amplitudes and travel times is provided by the study of McCreery (1986), who measured spectral amplitude fluctuations across the Wake Island hydrophone array of P waves from East Kazakh nuclear tests. McCreery found some correlation of small spectral amplitudes with early arrival times and large spectral amplitudes with late arrival times. The standard deviations of the travel time residuals, however, were larger than the difference in travel time residuals between small and large amplitude events.

An intuitive argument why log amplitudes do not precisely correlate with travel times can be made by considering travel time curves and ray density plots of test structures. It can be seen that the common situation is that rays will tend to cluster near caustic surfaces and regions of high velocity gradient. The rays having the slowest travel times, however, will tend to be slightly displaced from the regions of densest rays. An example of this can be seen in the fault zone calculations of Cormier and Spudich (1983). In that example, the highest amplitudes are associated with caustics near a region of high lateral gradient at the edges of the fault zone; the slowest travel times are in the center of the fault zone. Thus, log amplitudes will tend to be correlated only in a general regional sense with travel times. A travel time-log amplitude plot will typically have large scatter.

6

Coda stability and waveform complexity For variations in source and receiver site on the order of 10 to 100 km., magnitude measures based on integrated P coda vary less than those based on the amplitude of the first several cycles of the P wave (Ringdal, 1983; Baumgardt, 1985; Gupta *et al*., 1986). This observation is consistent with the effects of focusing and defocusing by large scale structures in the mantle beneath the source region together with the assumption that the coda is generated by scattering by heterogeneities concentrated in the crust and uppermost mantle. In the source region, the effects of focusing and defocusing are minimized for scatterers located at a distance from the source that is greater than the characteristic wavelength of heterogeneity in the mantle beneath the source (Figure 8). For a hypothesis of the coda being dominated by single scattering, the later part of the coda will become progressively better in minimizing the effects of focusing and defocusing. This is because the later coda, being generated by scattering structure further from the epicenter, is more likely to travel to the receiver by a P wave path that does not sample the mantle heterogeneity. In three-dimensional geometry, this effect is magnified by integrating the scattering that occurs within a concentric ring surrounding the source.

A simplified calculation of this effect for the Pahute structure is shown in Figures 9 and 10. The scattering is assumed to be dominated by scattering of energy propagating nearly horizontally in the crust as S, Lg, or Rg waves into P waves propagating nearly vertically away from the source region. A ring of scatterers is assumed at a radius of 33 km. from a Pahute source. The radius of the ring is chosen to simulate the effects on the coda arriving 10 sec. after the direct P wave for S, Lg, or Rg to P scattering. The group velocity of the S, Lg, or Rg wave is assumed to be 3.3 km./sec. Wide angle scattering is assumed in the vertical angle but only narrow angle scattering is assumed in the azimuthal angle. Scattering near the receiver, scattering in the deep mantle, and multiple scattering are neglected for the time being.

There is still a suggestion of the northerly minimum in amplitude in Figure 10, but the minimum is not as intense or as wide in azimuthal range as for the direct P wave. The nearly constant levels of amplitude in westerly azimuths for more distant stations are due to the fact that the scattered P rays traversed a portion of the model in which the reference one-dimensional model of the structure was unperturbed.

These effects are consistent with those observed by Lay and Welc (1986ab) in Pahute waveforms in the 5 to 10 sec. time window following the direct P. They found the coda to be less affected by defocusing in northerly azimuths. The effects decreased with later time in the coda. P waveforms were generally more complex in northerly azimuths. This agrees with one of the scenarios proposed for the origin of waveform complexity by Douglas *et al* (1973), in which complex waveforms are created when the direct P wave is defocused by mantle structure relative to the P coda.

Other examples of forward modeling of focusing and defocusing (Cormier, 1986, McLaughlin, 1987) find that variations in source location as small as 30 to 50 km. are sufficient to strongly affect the amplitudes of direct P waves. The controlling factor is the characteristic scale lengths of 1 per cent and greater velocity heterogeneities in the upper mantle. These observations bear upon a hypothesis of Douglas *et al* (1981). To account for complex and simple waveforms observed over nearly identical ray paths, Douglas *et al* suggested that the coda was generated by weak scattering all along the ray path rather than by scattering concentrated in the crust and uppermost mantle. The results of the focusing and defocusing experiments reported here and in other studies, however, suggest that it may not be necessary to invoke significant scattering in the deep mantle to account for simple and complex waveforms for nearby ray paths, if "nearby" is taken to be distances as large as 30 to 100 km.

Wide versus narrow angle scattering Wide angle scattering in the azimuthal angle can be more effective in reducing the effects of focusing and defocusing compared to narrow angle scattering. Wide angle scattering allows greater opportunities for

scattered P waves to sample regions outside of a particular focusing/defocusing structure in the upper mantle. From amplitude and phase correlations at NORSAR, Wu and Flatte (1986) suggest that wide angle scattering is particularly important in the upper 1 to 2 km. of the crust. They postulate that wide angle scattering at shallow depths can account for imperceptible fluctuations in travel time being associated with large amplitude fluctuations at small (7 km.) aperture sub-arrays (e.g., Thomson, 1983).

To the extent that greater scattering at wider angles occurs in the shallow crust, the teleseismic P coda of shallower explosions should be more stable and successful in minimizing and homogenizing the effects of focusing/defocusing structures in the mantle beneath the source. Different scattering properties of the shallow crust compared to the deep crust may account for the observation of greater complexity for smaller and shallower tests compared to larger and deeper events as reported by Lay and Welc (1986a). This correlation was generally found in P waveforms from tests at Novaya Zemlya, but was less apparent at other test sites.

Coda generated near the receiver Coda generated near the receiver is less successful in removing the effects of focusing/defocusing structure beneath the source region. This is illustrated in Figure 11, which plots a series of ray end points for different vertical and azimuthal take-off angles in the vicinity of a low amplitude (defocused) and high amplitude (focused) station. In both cases, the concentration of ray end points is quite uniform over a large area. This is because the small region in which rays are focused or defocused near the source is spread out over a very broad region after propagation to teleseismic range. Scattering can occur over a very broad region near the receiver for rays having a very small distribution of vertical and azimuthal take-off angles of direct P near the source. Assuming that scattering is uniformly concentrated in the crust and upper mantle near the earth's surface, the P coda for an explosion or earthquake near the earth's surface will be composed of roughly equal amounts of P energy scattered near the source and near the receiver. The P coda of a deep focus earthquake will primarily be composed of P energy scattered

9

near the receiver. These predictions have been verified by a comparison of the phase velocities of late P coda energy from deep and shallow earthquake sources (Dainty, 1986). With this model of scattering, it is clear why coda magnitudes of shallow events will tend to be only about fifty per cent successful in homogenizing the effects of focusing and defocusing structures near the source and receiver. At each receiver, a coda magnitude will be successful in removing the effects of focusing/defocusing structures beneath the receiver, with the performance progressively improving with increasing time into the coda. However, even the very late portion of the coda will not be totally successful in removing the effects of focusing/defocusing structure beneath the source. This is because about fifty per cent of the late coda will consist of direct P that has been focused or defocused near the source and then scattered near the receiver.

A true estimate of the fluctuation of coda amplitude due to focusing and defocusing structures near the source would look more like an average of Figure 3 and 10. This agrees with the results of many coda studies. Lay and Welc (1986a), for example, find a similar, although less pronounced, azimuthal pattern of amplitudes in the 10-15 sec time window of P coda as for direct P from Pahute events. The P coda also seems to be generally more stable than direct P, but not necessarily for every source and receiver combination (Bullitt and Cormier, 1984). The increased stability will depend on the relative importance of scattering and focusing/defocusing near the source versus that occurring near the receiver. The worst performance of coda magnitudes will occur in a situation in which the strongest focusing/defocusing is in the upper mantle close to the source and in which scattering in the crust near the source is relatively weak.

CONCLUSIONS

A known three-dimensional structure beneath Pahute Mesa, Nevada Test Site (Taylor, 1983) can account for many of the features in the azimuthal amplitude pattern of teleseismic P waves from Pahute underground tests. This model can be used to

correct for focusing and defocusing effects of the structure beneath Pahute Mesa accounting for factors of three in amplitude fluctuation and for 0.6 sec. in travel time fluctuation. The reduction in variance of teleseismic magnitude or log amplitude using these corrections is about 25 per cent, similar to the reduction of variance in teleseismic travel times. These results suggest that three-dimensional velocity inversions capable of resolving 10 to 20 km. scale length structure down to 100 km. depth may be useful in making corrections for focusing/defocusing structure in the mantle beneath other test sites. Velocity inversions that primarily resolve scale lengths larger than these, such as the studies by Minster *et al* (1981) and Montfort and Evans (1982), are much less useful in formulating amplitude corrections. By analogy to the Taylor inversion for NTS structure, the data required to resolve structure having these scale lengths would consist of origin times and locations of tests widely distributed over linear dimensions on the order of 100 km., with significant concentrations of tests spaced less than 10 km. apart. It is also necessary to obtain an average crustal structure within the test site from seismograms recorded at local and regional range.

The focusing and defocusing effects of 20 to 50 km. scale length structure having perturbation in P velocity of several per cent is nearly independent in the frequency band of teleseismic body waves. This conclusion is even stronger in the 0.2 to 10 Hz. band in which measurements are made on the teleseismic P waves of underground nuclear tests. Frequency dependent effects in the coda of teleseismic P waves are more likely due to frequency dependent effects in the scattering processes occurring near the source and receiver.

Magnitude measurements based on the integrated energy in the coda of teleseismic P waves are likely to be more stable because they can remove some of the focusing/defocusing effects of three-dimensional mantle structure near the source. The deeper the measurement is made in the coda, the less affected it will be by mantle structure near the source. The optimal time in the coda for this measurement should be as long as possible after the direct P wave given the signal to noise ratio. The

11

minimum time to achieve good stability can be estimated by dividing the length of characteristic scale lengths of mantle structure near the source by the velocity of the presumed scattered wave near the source. For example, assuming a 3.3 km./sec. S wave is scattered into a P wave that is propagated to teleseismic range, one would estimate that after 30 sec. into the coda, the focusing/defocusing effects of 100 km. scale and smaller length structure beneath the source would be minimized. Coda magnitudes, however, are only partially successful in removing the focusing/defocusing effects of structure beneath the source. They cannot remove these effects from the fraction of the coda that is due to scattering of direct P near the receiver.

These conclusions are consistent with tests of the relative performance of coda versus classical magnitudes. The predicted behavior of coda amplitude critically depends on assumptions about the distribution of mantle heterogeneity with depth. Smaller scale heterogeneities with greater per cent velocity fluctuations are assumed to be concentrated closer to the surface. Scale lengths on the order of several kilometers to 10 kilometers are assumed in the crust and scale lengths on the order of 10 to 100 kilometers are assumed in the upper mantle. Fluctuations in the mid and lower mantle down to the D" layer near the core are assumed to be smaller than 1 per cent.

ACKNOWLEDGEMENTS

REFERENCES

Archambeau, C.B. (1972). The theory of stress wave radiation from explosions in prestressed media. *Geophys J R Astr Soc*, *29*, 329-366.

Bache, T.C., (1976). The effect of tectonic release on short period P waves from NTS explosions. *Bull Seism Soc Am*, *66*, 1441-1457.

Baumgardt, D. (1985). Comparative analysis of teleseismic P coda and Lg waves from underground nuclear explosions in Eurasia, *Bull Seism Soc Am*, *72*, S319-S330.

Bullitt, J.T., and V.F. Cormier (1984). The relative performance of mb and alternative measures of elastic energy in estimating source size and explosion yield, *Bull Seism Soc Am*, *74*, 1863-1882.

Cerveny, V., (1985a). The application of ray tracing to the propagation of shear waves in complex media, in *Seismic Exploration*, eds. Treitel, S., and Helbig, K., Vol. on Seismic Shear Waves, ed. Dohr., G., Geophysical Press, pp. 1-124.

Cerveny, V., (1985b). Gaussian beam synthetic seismograms, *J Geophys*, *58*, 44-72.

Cormier, V.F., and P Spudich (1984). Amplification of ground motion and waveform complexity in fault zones: examples from the San Andreas and Calaveras faults, *Geophys J R astr Soc*, *79*, 135-152.

Cormier, V.F., (1986). An application of the propagator matrix of dynamic ray tracing: the focusing and defocusing of body waves by three-dimensional velocity structure in the source region. *Geophys J R Astr Soc*, *87* xxx-xxx.

Dainty, A.M. (1985). Coda observed at NORSAR and NORESS, Final Technical Report, AFGL-TR-85-0199, Hanscom AFB, 73pp.

Douglas A., P.D. Marshall, P.G. Gibbs, J.B. Young, and C. Blamey (1973). P signal complexity re-examined, *Geophys J R Astr. Soc.*, *33*, 195-221.

Douglas, A., J.A. Hudson, and B.J. Barley (1981). Complexity of short period P seismograms: What does scattering contribute? Report No. 03/81, Atomic Weapons Research Establishment, Aldermaston, Berkshire, United Kingdom.

Dziewonski, A.M., and D.L. Anderson (1981). Preliminary reference earth model (PREM), *Phys. Earth Planet. Inter.*, *25*, 297-356.

Gupta, I.N., R.R. Blandford, R.A. Wagner, J.A. Burnetti, and T.W. McElfresh (1985a). Uses of P coda for determination of yield of nuclear explosions, *Geophys J R Astr Soc*, *83*, 541-554.

Helmberger, D.V., and D.M. Hadley (1981). Seismic source functions and attenuation from local and teleseismic observations of the NTS events Jorum and Handley, *Bull Seism Soc Am*, 51-77.

Lay, T., T.C. Wallace, and D.V. Helmberger (1984). The effects of tectonic release on short period P waves from NTS explosions, *Bull Seism Soc Am*, *74*, 819-842.

Lay, T., and J.L. Welc (1986). Analysis of near-source contributions to early P-wave coda for underground explosions: 1. Waveform Complexity, *Bull Seism Soc Am.*, *76*, submitted, 1986.

Lay, T. (1986). Analysis of near-source contributions to early P wave coda for underground nuclear explosions: 2. Frequency Dependence, *Bull Seism Soc Am*, *76*, submitted, 1986.

Lynnes, C., and T. Lay (1984). Defocusing of short period P waves by a high velocity anomaly beneath Pahute Mesa. *EOS Trans Am Geophys Un.*, *65*, 994.

Minster, J.B., J.M. Savino, W.L. Rodi, J.F. Masso, and T.H. Jordan, (1981). Three-dimensional velocity structure of the crust and upper mantle beneath the Nevada Test Site, Final Technical Report, SSS-R-81- 5138, S-cubed, La Jolla, California.

McCreery, C.S., (1986). Yield estimation from spectral amplitudes of direct P and P coda recorded by the Wake Island deep ocean hydrophone array, preprint.

McLaughlin, K.L., and L.M. Anderson (1987). Stochastic dispersion of short-period P waves due to scattering and multipathing, *Geophys. J. R. Astr Soc*, in press.

Montfort, M.E., and J.R. Evans (1982). Three-dimensional modeling of the Nevada Test Site and vicinity from teleseismic P-wave residuals, Open-File Report 82-409, U.S. Geol. Survey, Menlo Park, California.

Ringdal, F. (1976). Maximum-likelihood estimation of seismic magnitude, *Bull Seism Soc Am.*,*66*, 789-802.

Ringdal, F., (1983). Magnitude from P-coda and Lg using NORSAR data, Fifth Annual DARPA Symposium on Seismic Detection, Analysis, Discrimination and Yield Determination, p. 34.

Taylor, S.R., (1983). Three-dimensional crust and upper mantle structure at the Nevada Test Site, *J Geophys Res*, *88*, 2220-2232.

Thomson, C., (1983). Ray theoretical amplitude inversion for laterally varying velocity structure below NORSAR, *Geophys. J. R. Astr. Soc.*, *74*, 525-558.

Wallace, T.C., D.V. Helmberger, and G.R. Engen (1983). Evidence for tectonic release from underground nuclear explosions in long period P waves, *Bull Seism Soc Am.*, *73*, 593-613.

Wallace, T.C., D.V. Helmberger, and G.R. Engen (1985). Evidence of tectonic release from underground nuclear explosions in long period S waves, *Bull Seism Soc Am*, *75*, 157-174.

Wu, R-S., and S.M. Flatté (1986). Transmission fluctuation and angular decorrelation of seismic P-waves across a large seismic array caused by the lithosphere modeled as a random medium (abstract), *EOS Trans Am Geophys Un*, *67*, 315.

FIGURE CAPTIONS

Figure 1. A representative epicenter of an underground nuclear test at Pahute Mesa is marked by the cross (x). Iso-P velocity contours at 100 km. depth are shown for a high velocity anomaly resolved in the study by Taylor (1983).

Figure 2. Teleseismic P waves synthesized by superposition of Gaussian beams for stations at 60° distance and variable azimuths for an explosive point source at 1 km. depth. The source location is shown in Figure 1. The numbers alongside each seismogram are measurements of peak to peak amplitude. A reference line, from which travel time variations may be measured from the minimum trough, is shown in the short period column.

Figure 3. Predicted amplitudes of teleseismic P waves as a function of azimuth. Amplitudes were calculated by dynamic ray tracing in the Taylor model and normalized by the spreading factor in a one-dimensional model at 60° distance.

Figure 4. Observed amplitudes of teleseismic P waves from Pahute Mesa tests as a function of azimuth from Lay et al (1984).

Figure 5. Predicted and observed amplitudes of the Pahute Mesa tests are plotted on an equal area, lower hemisphere projection, as

a function of vertical and azimuthal angles of the rays leaving the heterogeneous region at 100 km. depth. The radius of the focal sphere is taken to be that for the vertical take-off angle of core grazing P waves in a one-dimensional, radially symmetric earth. $\delta \log A$ measures the difference in log amplitude from the log amplitude predicted in a one-dimensional earth.

Figure 6. The difference in time T of teleseismic P waves propagating from a source located as shown in Figure 1 from the time T_{PREM} calculated in the radially symmetric earth model of Dziewonski and Anderson (1981).

Figure 7. Correlation of calculated amplitudes and travel times for teleseismic P waves from a Pahute Mesa source in the Taylor model.

Figure 8. Schematic ray paths of direct P and P coda energy for a source located near a velocity heterogeneity in the upper mantle. P, S, Lg, or Rg energy propagates in the direction of the dashed line away from the source and is scattered into a P wave by a heterogeneity in the crust or upper mantle.

Figure 9. An approximate calculation of focusing and defocusing effects is made for coda generated near the source by considering a ring of scatterers located 33 km. laterally from the source.

Figure 10. A focal sphere plot of the amplitude of coda arriving 10 sec. after direct P using the approximate calculation illustrated in Figure 9. The ring of scatterers was assumed to be centered around the epicenter shown in Figure 1. Symbols are defined in Figure 5. This calculation only simulates effects on coda generated near the source. The coda will also have a component generated near the receiver.

Figure 11. Ray end points are marked by crosses(x). Arrows are drawn for possible

scattering paths for coda generated near the receivers. The two stations were selected from the set used in the Gaussian beam calculations shown in Figure 2. The high amplitude station was the one at 135° azimuth and the low amplitude station is the one at 0° azimuth. Note that coda generated over a broad region near the receiver can be focused or defocused by structure near the source.
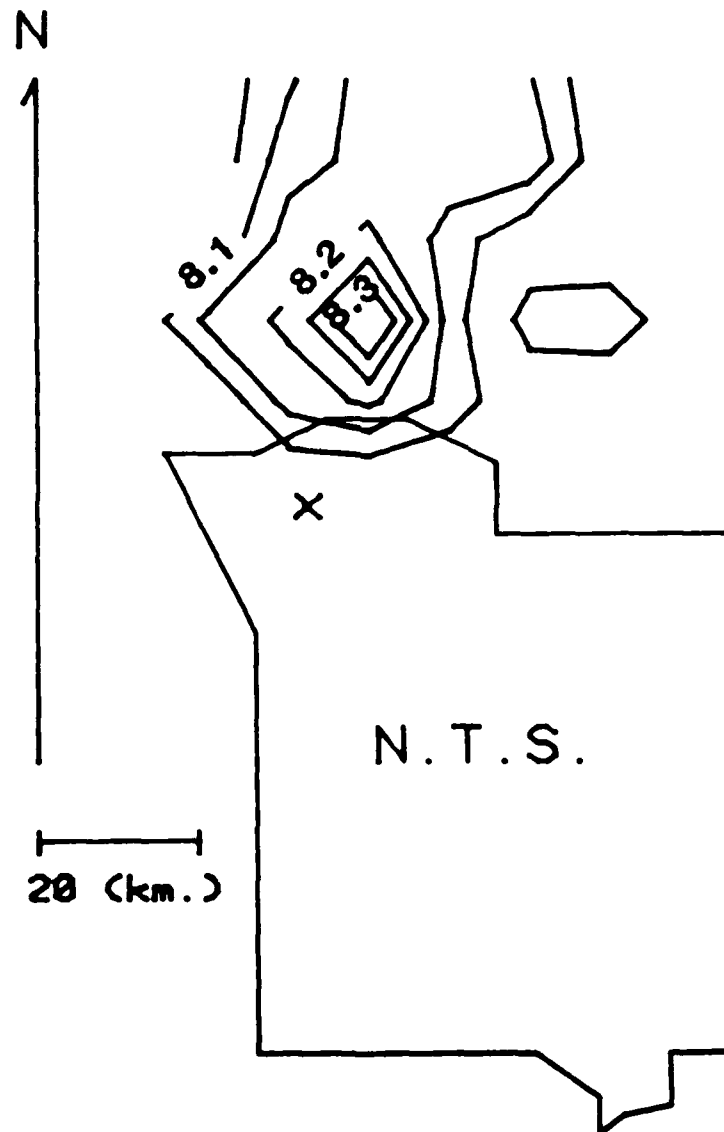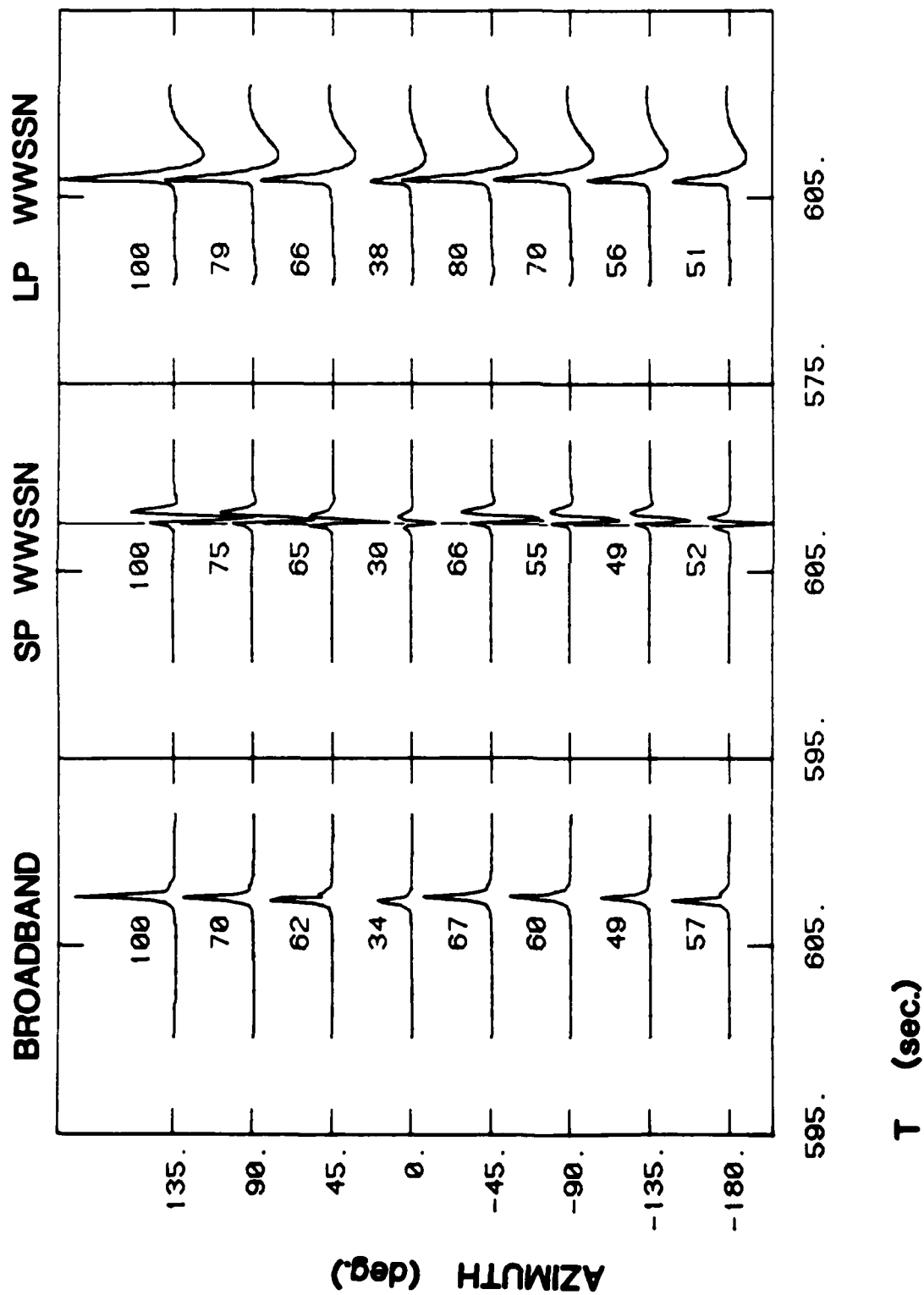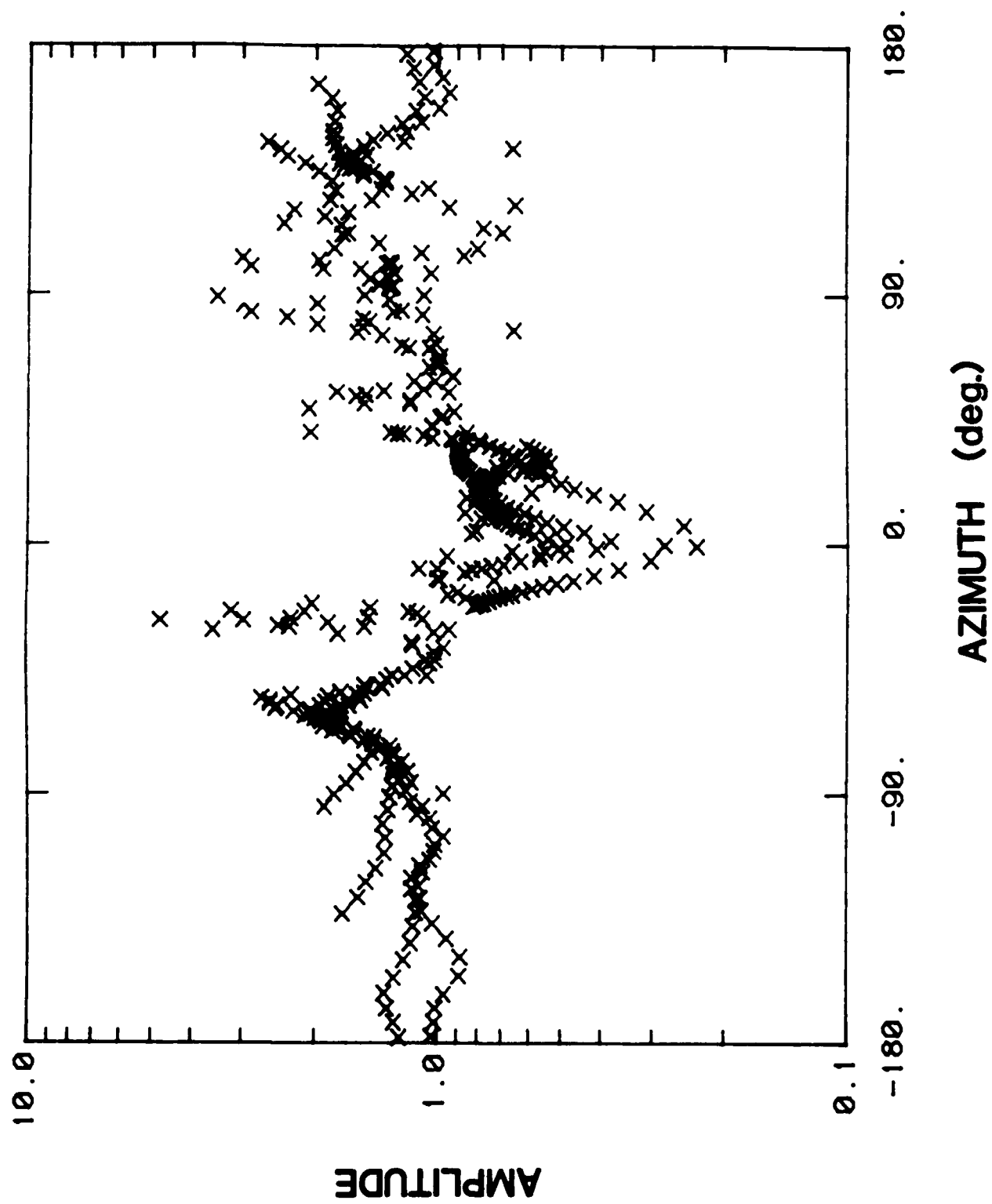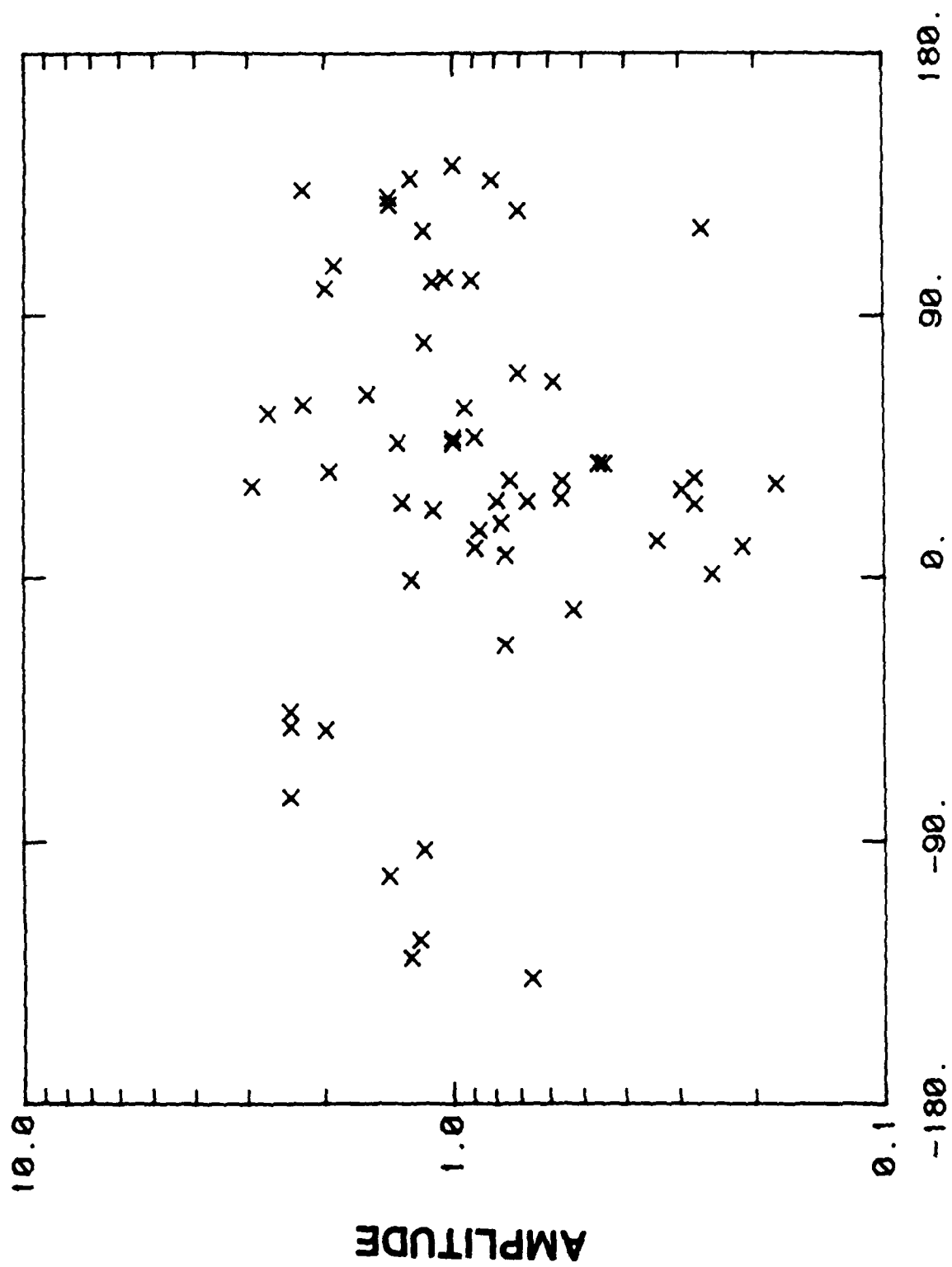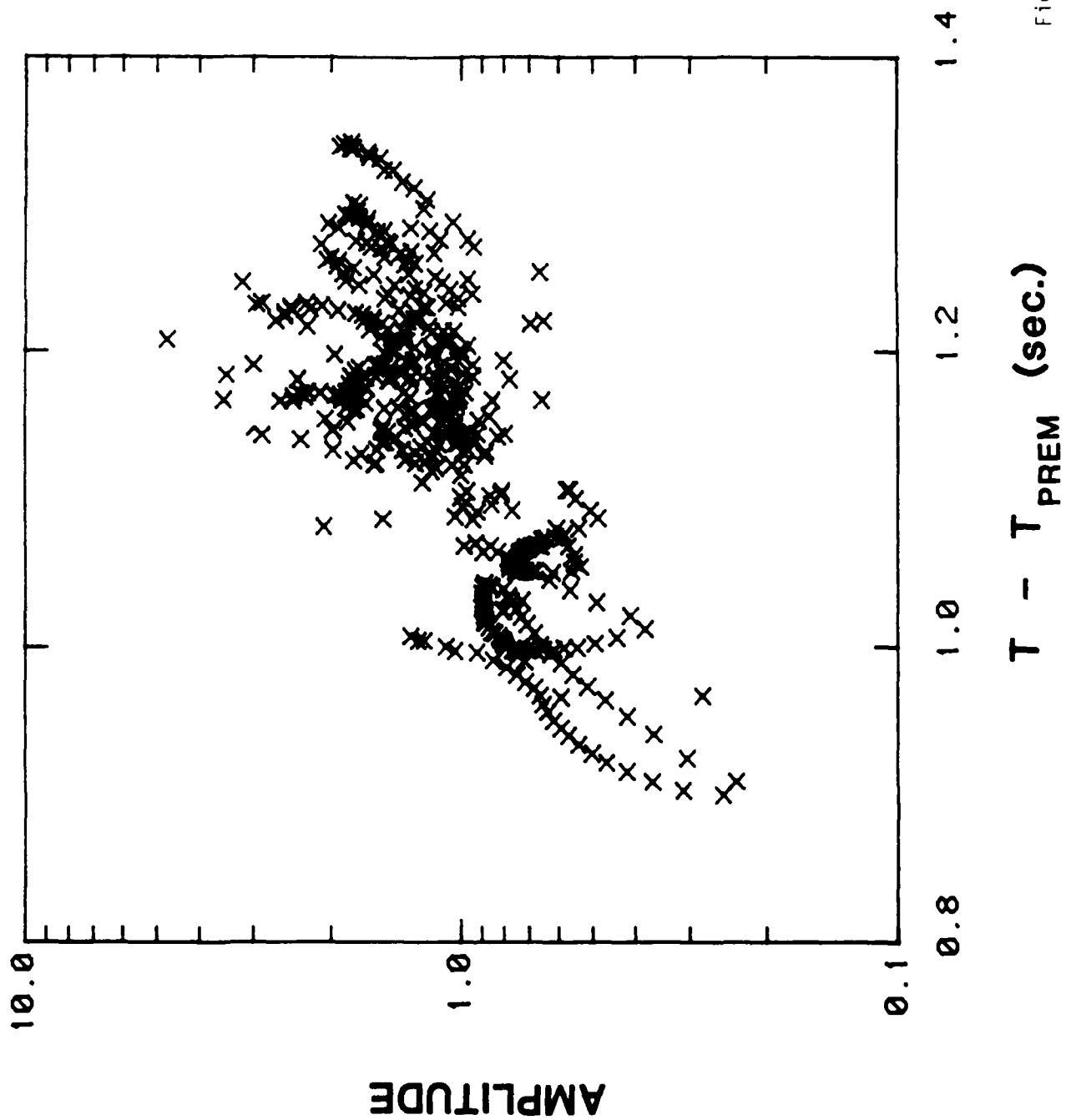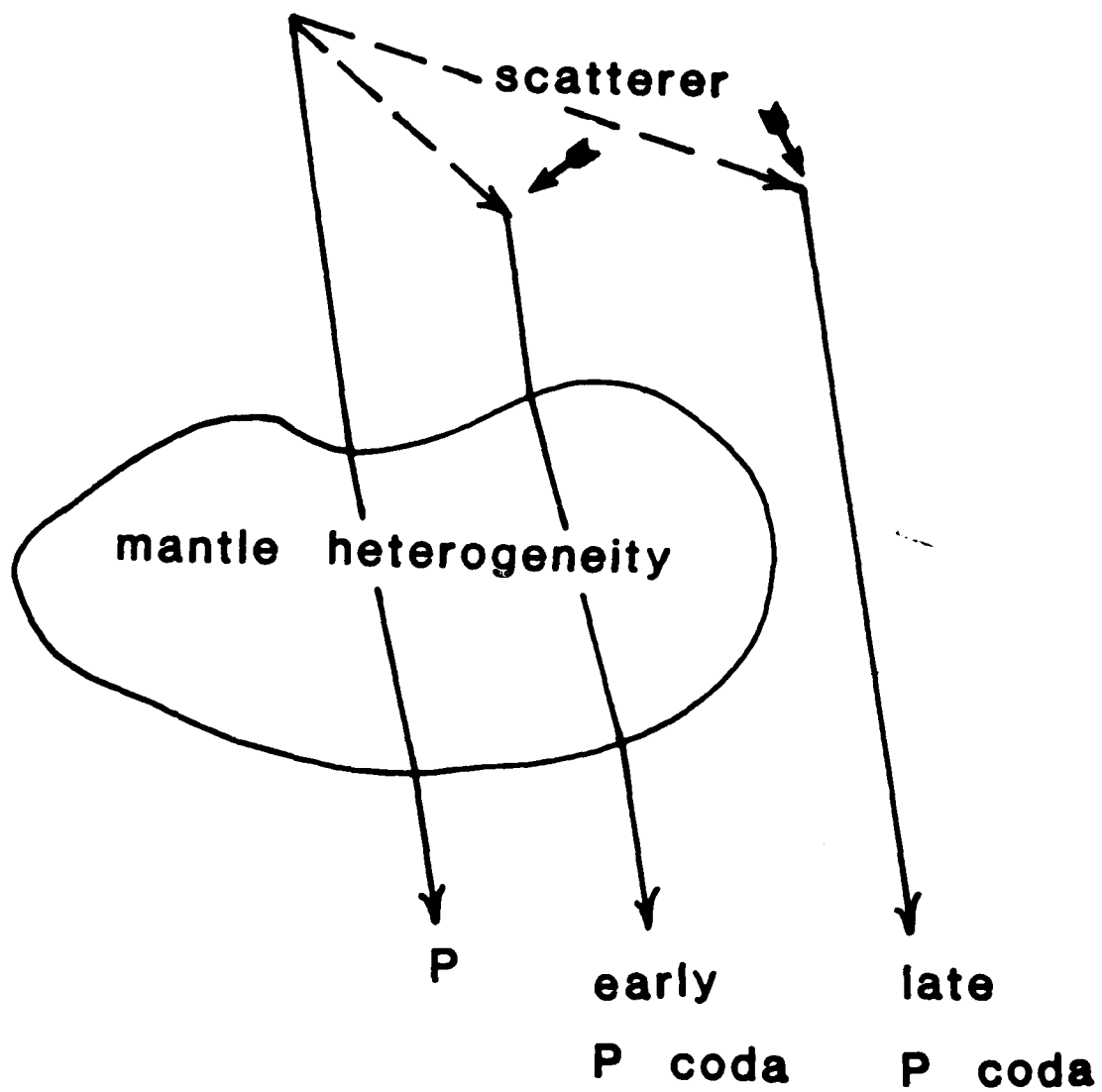
Figure 1

Figure 2

Figure 3

AMPLITUDE

AZIMUTH (deg.)

Figure 4

OBSERVED

PREDICTED

Positive

+ 0.0 < δlogA < 0.1 ◇

+ 0.1 < δlogA < 0.3 ◇

+ 0.3 < δlogA ◇

Figure 6.

21

Figure 6

Figure 7

scatterer

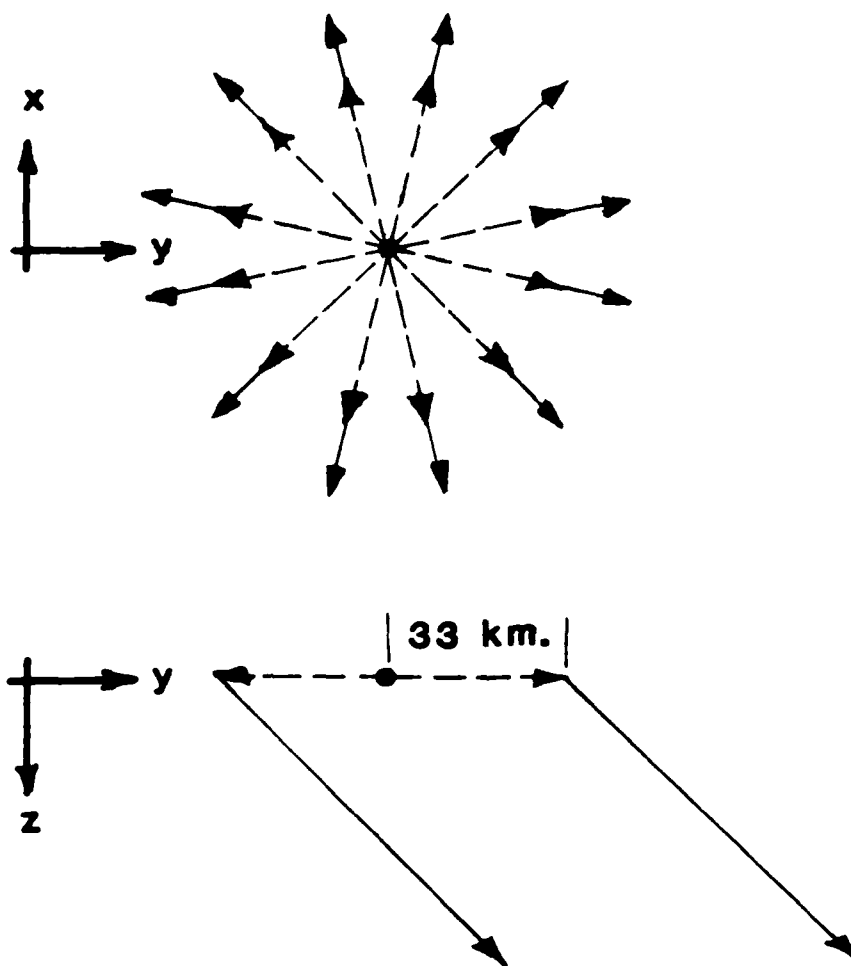mantle heterogeneity

P

early
P coda

late
P coda
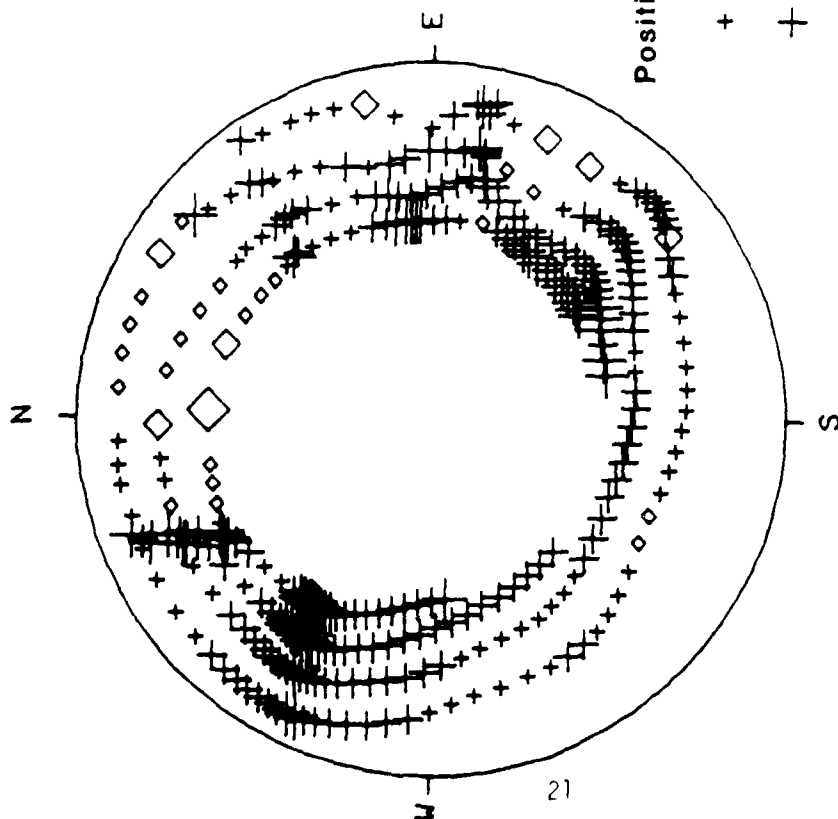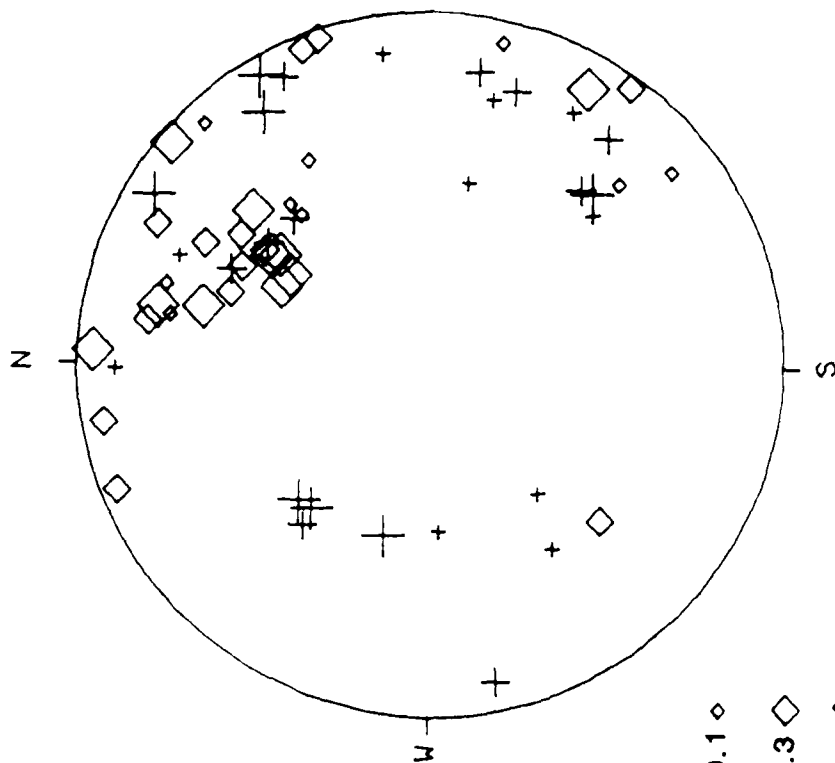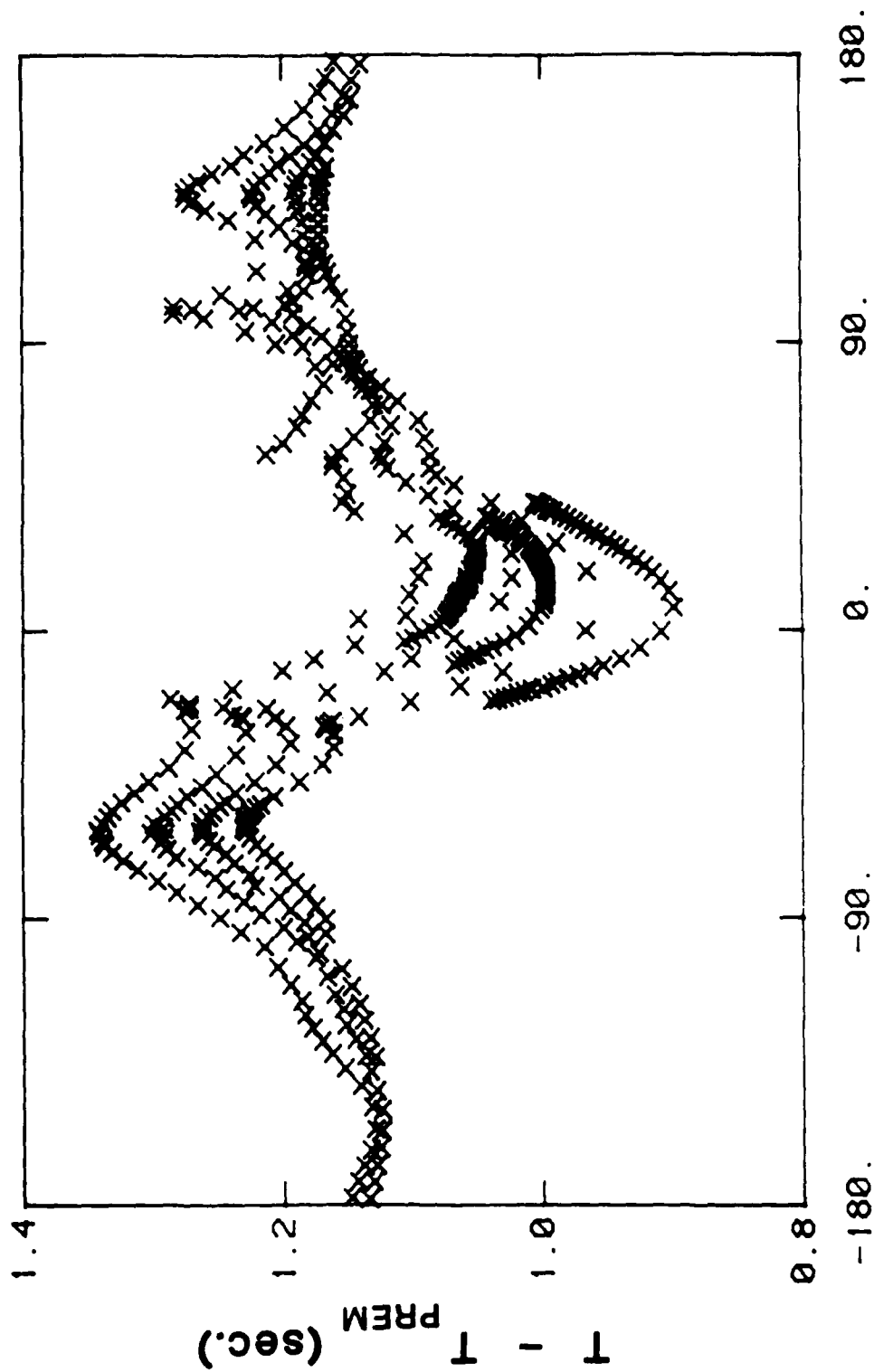
Figure 8

Figure 9

Figure 10
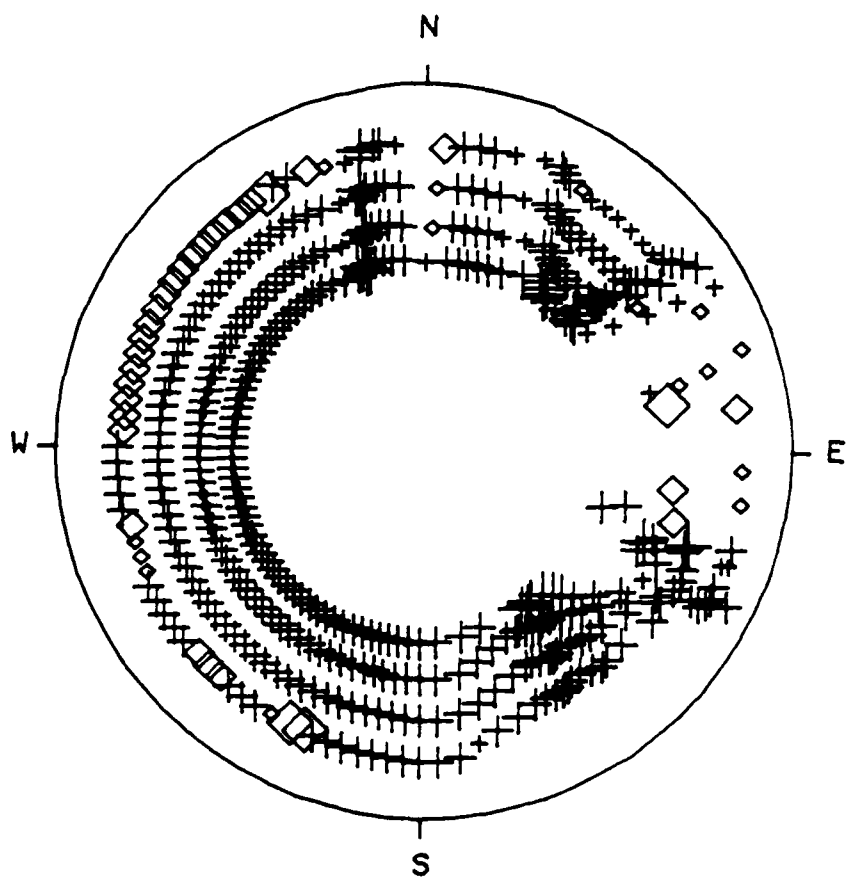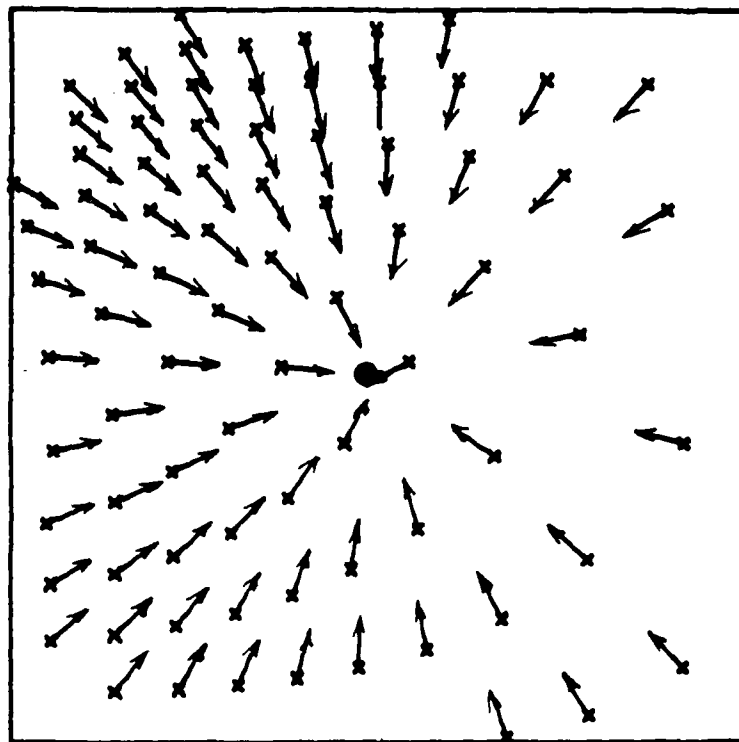
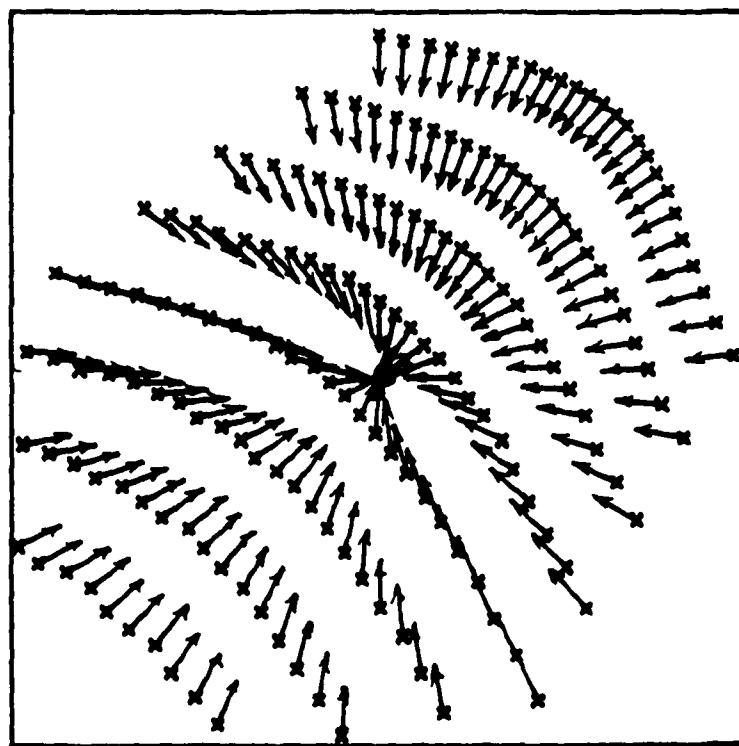LOW AMPLITUDE STATION

HIGH AMPLITUDE STATION

2000 (km.)

2000 (km.)

27

Figure 11

DATE
FILMED

5-28